496 *J. Phys. Chem. A* **1999,** *103,* 496−502

C−H Stretch Modes as a Probe of H-Bonding in Methanol-Containing Clusters

Christopher J. Gruenloh, Gina M. Florio, Joel R. Carney, Fredrick C. Hagemeister, and Timothy S. Zwier*

Department of Chemistry, Purdue University, West Lafayette, Indiana 47907-1393

Received: September 3, 1998; In Final Form: November 13, 1998

Resonant ion-dip infrared spectroscopy has been used to record infrared spectra of a series of benzene−(methanol)$_m$ clusters with $m = 1-5$ in the O−H and C−H stretch regions. Previous work has used the O−H stretch region as a probe of the H-bonding topologies of these clusters, from which it was deduced that benzene−(methanol)$_{1-3}$ contain H-bonded methanol chains and benzene−(methanol)$_{4-6}$ H-bonded methanol cycles. In the present work, the C−H stretch fundamentals of the methyl group of methanol and the aryl C−H groups of benzene are studied. While benzene's C−H stretch Fermi triad is virtually unchanged in frequency from one cluster to the next, the methyl C−H stretch vibrations undergo systematic wavenumber shifts characteristic of the H-bonding arrangement for each methanol in the cluster. Density functional theory calculations on the pure methanol and benzene−(methanol)$_m$ clusters faithfully reproduce the directions and approximate magnitudes of the observed shifts and provide a basis for assignment of the observed transitions to acceptor, donor, and acceptor−donor methanol subunits. The experimental results on the ν_2 fundamental of methanol in benzene−(methanol)$_{1-5}$ show characteristic frequency shifts due to (i) donor (D, -20 to -15 cm^{-1}), (ii) acceptor−donor (AD) and π donor (π) (-6 to -9 cm^{-1}), and (iii) OH···O acceptor/π donor (Aπ, -4 to $+2$ cm^{-1}). Calculations on (methanol)$_m$ and benzene−(methanol)$_m$ clusters extend the predictions to include characteristic shifts for (iv) double-acceptor/single-donor (AAD, $+5$ to $+15$ cm^{-1}), (v) single-acceptor (A, $+15$ to $+30$ cm^{-1}), and (vi) double-acceptor (AA) ($+20$ to $+30$ cm^{-1}). FTIR spectra of liquid methanol and of binary solutions of methanol with acetone-d_6, $CDCl_3$, and D_2O indicate that methanol's CH stretch frequency shifts reflect methanol's H-bonding environment in solution as well.

I. Introduction

Among the many probes of H-bonding, the magnitude and sign of the shifts in the frequencies of vibrational modes closely associated with H-bond formation have long served as important diagnostics of the presence and strength of H-bonding.[1] In methanol, for instance, the O−H stretch, which vibrates directly against the H-bond, undergoes a large shift to lower frequency when participating as a donor in an O−H···X H-bond.[1−6] The C−O stretch, one bond removed, shifts to higher or lower frequencies by up to 20 cm^{-1} depending on whether methanol acts as a donor or acceptor in H-bonding, respectively.[4,7−12]

In these cases, the normal modes experiencing the wavenumber shift show an obvious and direct linkage with the H-bond that perturbs it. On this basis, one would anticipate that the C−H stretch modes of methanol would be "spectator" modes toward H-bonding, serving as weak or unreliable indicators at best. Nevertheless, infrared and Raman studies in the condensed phase[7,8] have observed systematic changes in the C−H stretch modes that depend on the H-bonding environment. However, neither the correlation of these shifts with specific H-bonding arrangements nor a molecular-scale explanation of the observed behavior has yet been given, largely because the shifts present in condensed phase environments are the net result of a number of competing effects.

In the present paper, we use the unique attributes of gas-phase clusters to explore whether the C−H stretch modes in methanol can also serve as a probe of H-bonding, even though they are spatially removed from the H-bonding sites in methanol. The technique of resonant ion-dip infrared spectroscopy[13,14] is used to record the C−H stretch infrared spectrum of size- and conformation-selected benzene−(methanol)$_m$ clusters (hereafter referred to as BM$_m$). The O−H stretch spectra of the BM$_m$ clusters previously have provided an unambiguous assignment of the H-bonding topologies of the clusters.[6] As shown in Figure 1a), in BM$_1$, the methanol is a H-bond donor to benzene's π cloud, producing a 42 cm^{-1} shift to lower frequency in methanol's OH stretch fundamental. The methanol dimer and trimer in BM$_2$ (Figure 1b) and BM$_3$(Figure 1c) are longer H-bonded chains in which the terminal methanol retains and

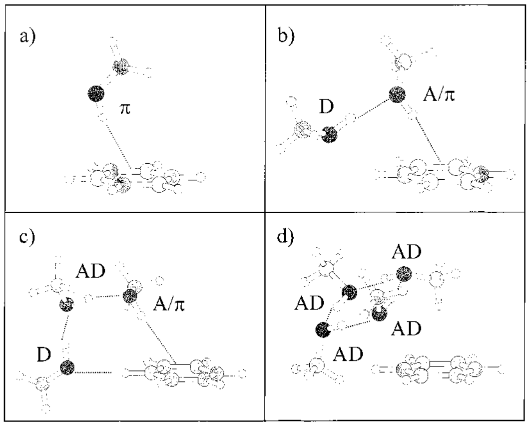

Figure 1. H-bonding topologies deduced for the BM$_{1-4}$ clusters from the OH stretch RIDIR spectra. The structures in (a)−(c) are those from the DFT Becke3LYP calculations while that in (d) is schematic only, since the orientation of the cyclic methanol tetramer relative to benzene is not known.

10.1021/jp983629l CCC: $18.00

strengthens its π H-bond to benzene. Beginning at $m = 4$, the BM_m clusters have M_m subclusters that are H-bonded cycles (with BM_4 shown schematically in Figure 1d) in which all methanols act simultaneously as acceptor and donor. Consequently, the BM_m clusters provide examples of π H-bonded (π), single donor (D), and acceptor/donor (AD), and acceptor/π (Aπ) methanols. Armed with a firm knowledge of the composition of the cluster and its basic H-bonding topology and assisted by Becke3LYP density functional theory (DFT) calculations[15−17] on the clusters, which faithfully reproduce the effect, we have uncovered a robust correlation between the observed C−H stretch frequency and the local H-bonding topology of each methanol in the cluster. In this paper, the pure methanol and BM_m clusters will serve as the basis for presenting the C−H stretch modes as secondary probes of H-bonding. In the paper on BW_nM_m clusters which follows,[18] the C−H stretch fundamentals are used in several cases to distinguish between possible isomers differing in the position of the methanol(s) in the mixed cluster.

II. Methods

A. Experimental Details. The experimental methods used in the present work have been described previously[19,20] and are only briefly reviewed here. The cold, gas-phase BM_m clusters are produced by supersonically expanding a mixture of the vapors of benzene and methanol in Ne-70 (70% neon and 30% helium) from a pulsed valve of 0.8 mm diameter operating at 20 Hz. The concentrations of the vapors are controlled by adjusting metered flows of Ne-70 over the liquid samples. Typical sample concentrations in the expansion are 0.2−0.4% benzene and 0.1−0.2% methanol in a balance of Ne-70 at a total pressure of 2 bar.

Resonant ion-dip infrared spectroscopy (RIDIRS) has been used to record C−H stretch infrared spectra of the BM_m clusters free from interference from one another. In this double-resonance scheme, first introduced by Page et al.,[13,14] the infrared transitions are observed indirectly as a dip in the R2PI ion signal with the UV laser tuned to the $S_1 \leftarrow S_0\ 6^1_0$ transition of the cluster of interest.[21] The mass-selected, one-color resonant two-photon ionization (R2PI) spectra of the clusters, which serve as a foundation for the present study, have been presented elsewhere.[22,23] BM_m clusters are resonantly ionized by the output of a Nd:YAG-pumped, doubled-dye laser operating at 20 Hz. Energies of 0.6−1.0 mJ of UV light/pulse are propagated through the ion source in a 1 mm collimated beam. In RIDIRS, the pulsed, near-IR output of a Nd:YAG-pumped optical parametric oscillator (OPO, 4−8 mJ/pulse, 2 cm^{-1} fwhm, focused by a 50 cm focal length CaF_2 lens)[19] is spatially overlapped with the UV laser used for R2PI but precedes it in time by about 200 ns. With the UV laser fixed on a selected cluster's 6^1_0 transition, the OPO is tuned, and any infrared absorption occurring out of the same ground state as that monitored in R2PI is detected as a depletion in the ion signal in the mass channel of interest. Active baseline subtraction[20] is used to remove long-term fluctuations in the baseline of collected spectra. By operating the pulsed valve and UV laser at 20 Hz and the OPO at 10 Hz, a gated integrator subtracts every other laser shot, one with and one without the infrared light present.

B. Calculations. The density functional theory (DFT) calculations of the structures, binding energies, and vibrational frequencies of the M_m and BM_m clusters of interest here have also been described previously.[5] The calculations employ the Becke3LYP functional with a 6-31+G* basis set.[15−17] This level of theory provides vibrational frequency shifts for H-bonded clusters in the OH stretch region that are in close correspondence with experiment and have provided a basis for assignment of the BM_m clusters to a given H-bonding topology. In that previous work,[5] the C−H stretch vibrational frequencies and infrared intensities were not included explicitly and so are presented here.

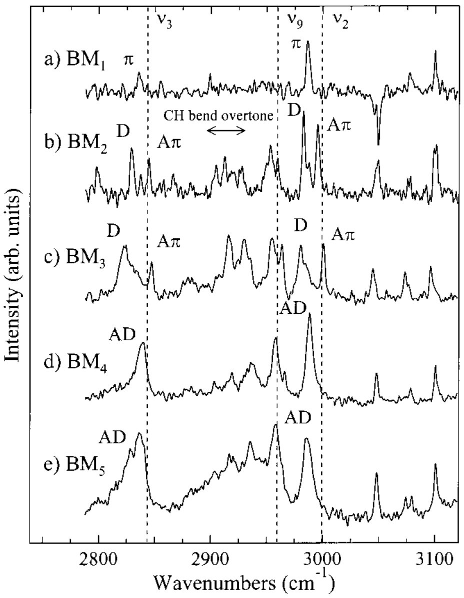

Figure 2. Resonant ion-dip infrared spectra of (a)−(e) BM_{1-5} in the CH stretch region. The vertical dashed lines mark the frequencies of the ν_2, ν_9, and ν_3 CH stretch fundamentals in methanol monomer. The labels correspond to the H-bonding types shown in Figure 1.

III. Results and Analysis

A. CH Stretch Transitions of Benzene And Methanol Monomers. The CH stretch bands of benzene monomer are found at 3048, 3079, and 3101 cm^{-1}. The only IR active CH stretch mode in benzene is $\nu_{20}(e_{1u})$. It mixes with $\nu_1 + \nu_6 + \nu_{19}$, $\nu_8 + \nu_{19}$, and $\nu_3 + \nu_6 + \nu_{15}$ to form a Fermi resonance tetrad, with the 3101 cm^{-1} transition an unresolved doublet at our resolution.[13]

All three CH stretch modes of methanol monomer are infrared active, having fundamental frequencies of 2999.4 (ν_2), 2959 (ν_9), and 2843.4 (ν_3) cm^{-1}, and are shown as dashed lines in Figure 2.[24−29] The ν_2 and ν_3 fundamentals of rigid methanol are of A′ symmetry in the C_s point group (staggered conformation), while ν_9 is of A″ symmetry. The form of the CH stretch normal modes for methanol monomer calculated using DFT Becke3LYP/6-31+G* are shown in Figure 3. The CH stretch region of methanol is complicated by the Fermi resonance these bands exhibit with the CH bend overtone and combination bands. These anharmonic couplings shift the CH stretch fundamentals and mix them with the bend overtones and combination bands, giving intensity to the bending levels. The harmonic DFT calculations ignore such couplings and hence do not reproduce the experimental positions of the CH stretch fundamentals accurately. Recently, Halonen[26] has calculated the CH stretch fundamental region, including anharmonic coupling with the bends. This work illustrates the effects that the CH stretch/bend coupling has on the energy level structure in the CH stretch ($v = 1$) region. On the basis of these calculations, it would appear that ν_2 is the most nearly pure C−H stretch band of the three.

The vibrational band origins are also shifted by the coupling of the stretch modes with hindered internal rotation, a full

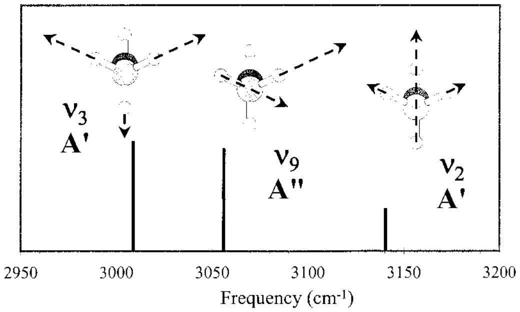

Figure 3. Calculated CH stretch vibrational frequencies, infrared intensities, and form of the normal modes for the methanol monomer using the DFT Becke3LYP level of theory with a 6-31+G(d) basis set. The calculations ignore Fermi resonance with the overtones and combination bands of the CH bend that influence the experimental positions and intensities of the bands.

TABLE 1: Experimental Fundamental Frequencies and Frequency Shifts (cm^{-1}) for the BM$_{1-5}$ Clusters in Methanol's CH Stretch Region

		frequency (cm^{-1})[a]		freq shift (cm^{-1})[b]	
cluster	H-bond type	ν_3	ν_2	$\Delta\nu_3$	$\Delta\nu_2$
BM$_1$	π	2835.5	2986.5	−7.9	−12.9
BM$_2$	D	2829.0	2982.6	−14.4	−16.8
	Aπ	2844.6	2995.5	+1.2	−3.9
BM$_3$	D	2823.0	2980.6	−20.4	−18.8
	AD	~2833	~2985	−10	−14
	Aπ	2847.2	3000.8	+3.8	+1.4
BM$_4$	AD	2839.7	2988.5	−3.7	−10.9
BM$_5$	AD	2836.9	2986.1	−6.5	−13.3

[a] Frequencies and frequency shifts are accurate to ±0.5 cm^{-1}. [b] Frequency shifts are taken relative to the ν_2 and ν_3 fundamentals of methanol monomer (ν_3 = 2843.4 cm^{-1}, ν_2 = 2999.4 cm^{-1}).

description of which is just beginning to emerge from recent high-resolution studies of Perry and co-workers.[24,25]

B. CH Stretch Transitions of Benzene in BM$_m$. Figure 2a−e presents the RIDIR spectra of the BM$_m$ clusters with m = 1−5 in the C−H stretch region, respectively. As anticipated above, the spectrum neatly divides between the aryl CH stretch bands of benzene (3040−3110 cm^{-1}) and methanol's methyl CH stretch bands (2800−3000 cm^{-1}). For all the BM$_m$ clusters except m = 3, the aryl C−H stretch bands appear unshifted in frequency, within experimental error (±1 cm^{-1}), from their value in free benzene. The BM$_3$ bands are uniformly shifted 5 cm^{-1} to lower frequency, presumably due to the effect of the methanol at the donor end of the M$_3$ chain (Figure 1c), which interacts with the CH group(s) on benzene. The ion gain signal present in the 3048 cm^{-1} transition of BM$_1$ is an artifact due to the fact that the BM$_1$ RIDIR spectrum was recorded in the benzene parent mass channel. While this maximizes the ion signal due to the BM$_1$ cluster (which fragments efficiently following photoionization), it opens the possibility for interference from IR-excited benzene monomer.

C. CH Stretch Transitions of the Methyl Groups in BM$_m$. Much more interesting are the methyl CH stretch bands of methanol molecules in the clusters. As can be seen from the RIDIR spectra of Figure 2, the BM$_m$ clusters show transitions that are readily assigned as ν_2, ν_3, and ν_9 CH stretch fundamentals. The Fermi resonant CH bend structure appears primarily as a clump of bands on the low-frequency side of ν_9, as marked in Figure 2b. Table 1 lists the experimental ν_2 and ν_3 CH stretch peak positions of BM$_m$ clusters with m = 1−5 at the present resolution (2 cm^{-1}). The spectra of BM$_4$ and BM$_5$ most clearly divide into ν_2, ν_3, and ν_9 subregions, since in these clusters the ν_2, ν_3, and ν_9 CH stretch fundamentals of all methanols in the cluster appear as a single, unresolved band of each type. The spectra due to the BM$_2$ and BM$_3$ clusters are more complex, but a close inspection (particularly of the ν_2 and ν_3 regions) shows that, even here, the individual transitions faithfully mirror one another, with each ν_2 transition being flanked by a corresponding ν_3 transition 152 ± 3 cm^{-1} lower in frequency.

In BM$_1$, the ν_9 and CH bend overtone structure is not easily observed at the present signal-to-noise level. Nevertheless, the ν_2 and ν_3 bands are present, arising from the single methanol in the cluster, which is π H-bonded to benzene. They appear with frequency shifts of −13 and −8 cm^{-1} from their positions in free methanol, respectively (Table 1). The close correspondence and simplicity of the BM$_4$ and BM$_5$ CH stretch spectra undoubtedly reflect the common H-bonding environment of all methanols in these clusters, since each molecule acts as single acceptor/single donor (AD) in cyclic M$_m$ subclusters. The ν_2 frequency shifts of these AD molecules are −11 and −13 cm^{-1} in BM$_4$ and BM$_5$, respectively, close to that of the π H-bonded methanol in BM$_1$.

The ν_2 and ν_3 transitions in BM$_2$ each appear as doublets split to the high- and low-frequency side of the corresponding π and AD bands in BM$_1$, BM$_4$, and BM$_5$ (Table 1). As shown in Figure 1b, one of the methanol molecules in BM$_2$ acts as a H-bond donor (D) to the other methanol, which accepts this H-bond and donates its O−H in a weak H-bond with benzene's π cloud (Aπ). This suggests that the opposing shifts of these transitions reflect their unique positions in the H-bonded structure of BM$_2$.

In a similar way, the ν_2 and ν_3 regions in BM$_3$ shows bands to the high- and low-frequency side of the π and AD band positions (Table 1). This separation is further than in BM$_2$ with the low-frequency band in each case exhibiting a shoulder on its high-frequency side (at about −13 cm^{-1}). In BM$_3$, the three methanols are in unique H-bonding positions in the M$_3$ chain, as donor (D), acceptor/donor (AD), and acceptor/π (Aπ). Once again, a plausible interpretation of the observed transitions is to assign each unique ν_2 and ν_3 transition to one of the methanols in the BM$_3$ chain structure.

To gain a better understanding of the observed frequency shifts, the experimental results can be compared with the vibrational frequency shifts calculated for the M$_m$ and BM$_m$ clusters from our previous study.[5] In that work, harmonic vibrational frequencies and infrared intensities were calculated for 13 structural isomers of M$_m$ clusters with m = 1−5 and also for the lowest-energy structures of BM$_m$ clusters with m = 1−3. Represented in this sample were methanol molecules occupying O−H···O donor (D), O−H···O acceptor (A), O−H···π donor (π), OH···O acceptor−donor (AD), OH···O acceptor−π donor (Aπ), OH···O double-acceptor (AA), and OH···O double-acceptor−donor (AAD) H-bonding sites. Table 2 lists the absolute frequencies and frequency shifts of the CH stretch modes for all the studied M$_m$ structural isomers with m = 1−4. The short-hand notation used to describe the various isomers is of the form $n + m_i$ or $(n) + m_i$ where n and (n) refer to a H-bonded chain or cycle of size n, respectively, and m_i is a branch of length m attached to the cycle or chain at position i.[5]

As is evident from the table, the frequency shifts computed for the bands fall into characteristic frequency shift ranges depending on the H-bonding environment experienced by each methanol. Figure 4a−e presents stick diagrams for the CH stretch modes of BM$_{1-3}$, M$_4$, and M$_5$, respectively. Only the ν_2 and ν_3 vibrations are included since these are least overlapped with the CH bend overtone structure in the experimental spectra.

TABLE 2: Calculated Methyl C−H Stretch Frequencies in M_n (n = 1−4) and BM_n (n = 1−3) Clusters

cluster			frequency (cm^{-1})[a]		freq shift (cm^{-1})	
size	type[b]	H-bond type	ν_3[c]	ν_2[c]	ν_3	ν_2
M_1		none	3011.03	3142.13	0.00	0.00
M_2		D	2994.96	3120.53	−16.07	−21.60
		A	3037.16	3157.08	26.13	14.95
M_3	(3)	AD	3014.79	3131.54	3.76	−10.59
		AD	3016.91	3133.41	5.88	−8.72
		AD	3020.43	3134.17	9.40	−7.96
	$\underline{3}$	D	2995.17	3115.25	−15.86	−26.89
		AD	3018.30	3133.78	7.27	−8.35
		A	3034.82	3166.81	23.79	24.68
	$\underline{2} + 1_1$	D	2996.94	3125.83	−14.09	−16.31
		D	2998.47	3126.29	−12.56	−15.84
		AA	3054.25	3170.19	43.22	28.05
M_4	(4)	AD	3016.71	3128.84	5.68	−13.29
		AD	3017.17	3129.30	6.14	−12.83
		AD	3017.45	3129.36	6.42	−12.77
		AD	3020.47	3129.45	9.44	−12.68
	$\underline{4}$	D	2994.20	3113.34	−16.83	−28.79
		AD	3010.63	3126.54	−0.40	−15.59
		AD	3027.50	3130.55	16.47	−11.58
		A	3032.16	3161.59	21.13	19.46
	$(3) + 1_1$	D	2982.47	3117.36	−28.56	−24.77
		AD	3020.82	3138.39	9.79	−3.74
		AD	3023.30	3139.43	12.27	−2.70
		AAD	3035.70	3151.21	24.68	9.08
	$\underline{3} + 1_1$	D	2993.35	3123.93	−17.68	−18.20
		D	2998.29	3119.08	−12.74	−23.05
		AD	3021.48	3138.62	10.45	−3.51
		AA	3049.00	3175.52	37.97	33.39
	$\underline{3} + 1_2$	D	2985.84	3116.79	−25.19	−25.34
		D	3007.13	3122.38	−3.90	−19.75
		AAD	3035.29	3149.74	24.26	7.61
		A	3038.65	3169.29	27.62	27.16
BM_1		π	3006.9	3131.8	−4.15	−10.33
BM_2		D	2996.8	3119.2	−14.27	−22.91
		Aπ	3029.8	3146.0	18.79	3.90
BM_3		D	2995.7	3113.1	−15.32	−28.99
		AD	3017.8	3130.4	6.75	−11.77
		Aπ	3034.9	3145.9	23.83	3.79

[a] Unscaled harmonic frequencies at the DFT Becke3LYP/6-31+G* level of theory. [b] $n + m_p$ is a H-bonded chain of length n with a branch of length m at methanol position p. $(n) + m_p$ is the corresponding notation for a cycle of size n. [c] The third CH stretch mode, ν_9, is not included due to its close proximity to the CH bend overtones in experiment.

Quantitative comparison will concentrate on the ν_2 frequency shift since this mode is calculated by Halonen to be least effected by Fermi resonance coupling and hence most nearly pure CH stretch in character.[26]

Table 2 also includes the corresponding frequency shifts for the CH stretch modes in BM_{1-3}. Calculations on the larger BM_m clusters were not carried out due to the size of the calculations and difficulties in optimizing these clusters containing cyclic M_m subunits, which interact only weakly with benzene. Perturbations on the CH stretch frequencies of the cyclic M_m clusters by benzene are anticipated to be small. The comparison of the experimental and calculated frequency shifts for BM_{1-3} indicates that the harmonic vibrational frequency calculations accurately reproduce the observed shifts.

The calculated results provide a basis for assignment of the observed CH stretch transitions in BM_2 and BM_3 (Figure 2b,c). As the labels in Figure 2 and 4 show, the bands with largest red shift in BM_2 and BM_3 are due to the donor methanol at the end of the methanol chain. The bands with smallest shift are due to the Aπ methanols at the other end of the M_2 and M_3 chains. In BM_3, we tentatively assign the shoulders on the high-frequency side of the donor bands as the AD methyl CH stretch due to the middle methanol in the M_3 chain.

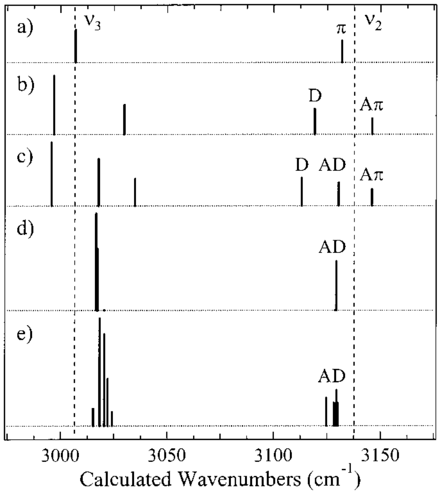

Figure 4. DFT Becke3LYP 6-31+G(d) calculations of the ν_2 and ν_3 CH stretch harmonic vibrational frequencies and infrared intensities in (a)−(c) BM_{1-3}, (d) M_4, and (e) M_5. The calculated ν_2 and ν_3 vibrational frequencies for the free methanol monomer are indicated by vertical dashed lines. See Figure 1 for the meaning of the π, D, Aπ, and AD labels. The CH stretch modes are largely local modes of the indicated methanols.

The corresponding CH stretch spectra of mixed benzene−(water)$_n$−(methanol)$_m$ clusters will be taken up in the adjoining paper.[18] There the methyl CH stretch bands will be used as the basis for distinguishing among isomers that differ in the position of the methanol molecule(s) in the same H-bonding structure (chain or cycle, for instance). Here it should simply be noted that in these mixed clusters, the CH stretch bands of methanol retain frequency shifts characteristic of their local H-bonding environment even though water is substituted for methanol in other positions in the cluster structure. For instance, when methanol acts as the H-bond acceptor in the water−methanol mixed dimer (W→M), the frequency shift calculated for ν_2 is within 1 cm^{-1} ($\Delta\nu = +16.4$ cm^{-1}) of the value for the acceptor methanol in methanol dimer ($\Delta\nu = +15.0$ cm^{-1}). Similarly, as a donor in M→W, its ν_2 band has a calculated frequency shift of -20.6 cm^{-1}, compared to -21.6 cm^{-1} in M_2.

IV. Discussion

The major conclusion to be drawn from this work is that the methyl CH stretch IR fundamentals of methanol undergo frequency shifts characteristic of their local H-bonding environment. As a result, the C−H stretch modes of methanol can be used as a probe of that H-bonding environment, much as the OH stretch modes of water and alcohols have in the past. In solution, shifts in the CH stretch vibrational frequencies have been noted,[7,8] but the complicated solvation structure and dynamics have hindered a clear molecular-scale interpretation of the effects. The ability of RIDIRS to record infrared spectra of cold, gas-phase clusters of a single size and molecular conformation free from interference from one another has provided a route to such a molecular-scale interpretation. The sensitivity of the OH stretch vibrations to H-bonding produced a firm assignment of the H-bonding structure of the clusters from the OH stretch RIDIR spectrum. Once in hand, the CH stretch region could then be analyzed in detail to search for the much smaller systematic shifts in the bands that accompany changes in the H-bonding topology of the clusters. Such shifts

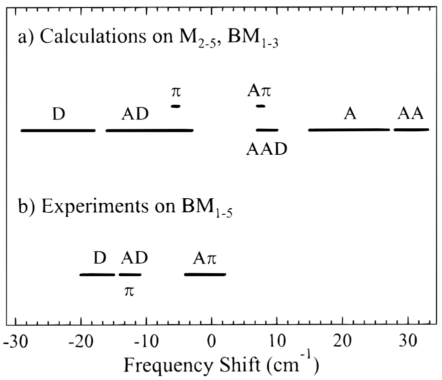

Figure 5. Pictorial summary of the CH stretch shifts of the ν_2 fundamentals (a) from calculations on M_{2-5} and BM_{1-3} and (b) from the experimental results on BM_{1-5}. Note the characteristic frequency shifts for the ν_2 CH stretch that reflect each methanol's H-bonding environment.

TABLE 3: Calculated Methyl Group Structural Changes in Methanol Induced by Methanol−Methanol H-Bonding[a,b]

methanol type	R_{CH} (Å)	θ_{OCH}(deg)[c]	ΔR_{OCH}(Å)[d]	$\Delta\theta_{OCH}$ (deg)[d]
monomer	1.0929	106.4400	0	0
	1.1000	112.0974	0	0
	1.100	112.0974	0	0
donor in	1.0941	107.1043	+0.0012	+0.6643
methanol dimer	1.1012	112.2109	+0.0012	+0.1135
	1.1012	112.2175	+0.0012	+0.1201
acceptor in	1.0918	106.3071	−0.0011	−0.1329
methanol dimer	1.0973	111.5544	−0.0027	−0.5430
	1.0973	111.1607	−0.0027	−0.9367
double acceptor	1.0911	106.1901	−0.0018	−0.2499
in T-shaped	1.0954	110.7742	−0.0046	−1.3232
methanol trimer	1.0954	110.7742	−0.0046	−1.3232

[a] All calculations were carried out using DFT Becke3LYP with a 6-31+G* basis set. [b] In all cases the optimized methyl group orientation is staggered relative to OH. The unique CH bond lengths and bond angles are those of the CH in the plane of the OH group. [c] The OCH bond angle for each H in the methyl group. A larger value of θ is associated with a closing of the methyl umbrella. [d] Relative to the monomer.

are indeed present, despite the fact that the methyl groups in these clusters are not directly involved in the intermolecular H-bonding.

As summarized in Figure 5, the combined experimental (Figure 5b) and calculated (Figure 5a) results reveal characteristic shifts of the CH stretch modes binding at each of the three hydrogen bonding sites on methanol (two acceptor sites on oxygen and one donor site at OH). The BM_m clusters include methanols that are involved as π H-bond donor (BM_1), OH···O donor ($BM_{2,3}$), OH acceptor/π donor ($BM_{2,3}$), and OH···O acceptor/donor methanols (BM_{3-5}). The calculations on M_m and BM_m clusters (Figure 5a) faithfully reproduce the experimental shifts for these H-bonding site types and extend the range of H-bonding site occupation to include A, AA, and AAD methanols. When methanol is involved in H-bond donation, the methyl CH stretch modes shift characteristically to lower frequency. The magnitude of the shift is dependent on the strength of the H-bond: when donation is to the weaker π H-bond, the shifts are small (-13 cm^{-1}), while donation to another methanol produces larger shifts (-17 to -19 cm^{-1}), which are cooperatively strengthened as the size of the H-bonded chain grows. When methanol accepts a H-bond, it is shifted to higher frequencies by similar amounts ($+15$ to $+25$ cm^{-1}). When it acts simultaneously as donor and acceptor, largely compensating effects lead to small shifts (-10 to -14 cm^{-1} experimentally) similar to those of the π H-bonded methanol. Finally, the calculations indicate that the CH stretch modes of double-acceptor methanols (AA) experience roughly twice the blue shift ($+28$ to $+33$ cm^{-1}) of single-acceptors, while AAD methanols are near in frequency to the single-acceptor methanols ($+7$ to $+9$ cm^{-1}), suggestive of a nearly additive effect for the frequency shifts associated with H-bonds at each of the three H-bonding sites on methanol (two acceptor sites on oxygen and one donor OH).

The fact that the experimental frequency shifts are reproduced by simple, harmonic vibrational frequency calculations indicates that the changes in frequency are a response of the methyl group to the differing intermolecular potentials felt by methanols with differing H-bond site occupation. In the absence of the calculations (at least) two other possibilities involving anharmonic coupling would need to be considered as well.

One such alternative would be to ascribe the CH stretch band shifts to changes in the Fermi resonant coupling with the CH bend overtones and combinations. In this scenario, the differing frequencies of the bands in BM_m could have been a response to changes in the magnitude or sign of the Fermi resonance coupling with the CH bends. However, if this were the case, one would anticipate significant changes in the separation between ν_2, ν_3, and ν_9 to accompany these changes, which is not observed. Instead, a simple shift of the bands at constant separation is observed.

A second alternative would ascribe the characteristic shifts to changes in the barrier to internal rotation of the methyl group by the H-bonding environment of the methanol.[30] This could indirectly produce frequency shifts in the CH stretch modes, since the magnitude of the hindering barrier should be sensitive to the length of the CH bonds. We have calculated the barriers to methyl internal rotation in methanol−water dimers in which methanol acts as donor and acceptor, respectively, in the form of a relaxed potential energy surface scan. At all levels of theory explored (DFT/Becke3LYP/6-31+G*, HF/6-31+G*, MP2/6-31+G*), the barrier to methyl rotation is lowered by about 25% (10%) when methanol is in the donor (acceptor) position. Since the direction of the barrier change is the same in both donor and acceptor positions, it seems unlikely that the changing methyl rotor barrier could account for the differing directions of the shifts observed experimentally. Furthermore, the harmonic frequency calculations ignore such effects and yet reproduce the experimental shifts.

We conclude, then, that the major source of the observed frequency shifts is simply the changes these different H-bonding environments have on the C−H stretch force constant, reflecting changes in the shape of the C−H bonds' intramolecular potential. In the model of solution frequency shifts put forward by Buckingham,[31−33] the frequency shift in mode i, $\Delta\nu_i$, induced by solvation is proportional to

$$\Delta\nu_i \propto \left(\frac{\partial U}{\partial Q_i}\right)$$

where U is the intermolecular potential and Q_i is the ith normal mode. In the present context, the frequency shifts reflect the intermolecular potential associated with a specific H-bonding configuration. When methanol is a H-bond donor, the electron density in the vicinity of the methyl group is increased; when it accepts a H-bond, it is decreased. According to the DFT calculations, accompanying these changes in methyl group charge distribution is a corresponding change in the C−H bond lengths and O−C−H bond angles, as summarized in Table 3. We see that the red shift (blue shift) of the donor (acceptor)

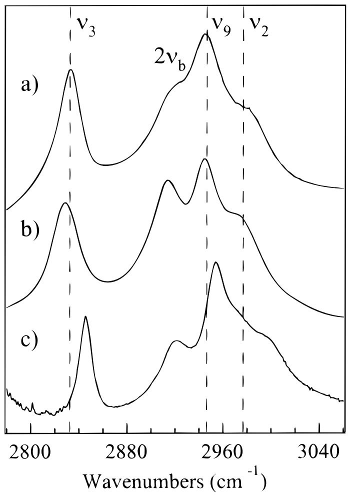

Figure 6. FTIR spectra in the CH stretch region of methanol for (a) pure liquid methanol at 22 °C, (b) 0.09 mole fraction methanol in acetone-d_6, and (c) 0.07 mole fraction methanol in D_2O. The assignments for the bands are made by comparison to those for the methanol monomer,[24−29] as confirmed by the BM_m cluster data in this work. Note the shifts of the ν_2 and ν_3 bands of methanol to (a) lower frequency and (b) higher frequency upon dilution in acetone-d_6 or D_2O, respectively. See the text for further discussion.

methanol C−H stretch is associated with an increase (decrease) in C−H bond length and an increase (decrease) in O−C−H bond angle.

The C−H stretch frequency shifts carry over with little change into the condensed phase, providing another signature of the average H-bonding environment of methanol in solution. As Figure 6a) shows, the methyl C−H stretch region of pure liquid methanol bears a close resemblance to the spectra of BM_4 and BM_5 (Figure 2d,e) in which the methanols are in a H-bonded cycle as AD methanols. The one-for-one correspondence lends support to an assignment of the observed peaks in the liquid-phase spectrum as labeled in the figure, though none of the modes is pure CH stretch. It appears that the Fermi resonance interactions present in methanol monomer are not too greatly perturbed in liquid methanol. Since pure liquid methanol is thought to be composed primarily of winding, H-bonded methanol chains, most methanol molecules in the liquid have an AD H-bonding site occupation.[34] Consistent with this, the ν_2 and ν_3 CH stretch fundamentals are shifted by −18 and −11 cm^{-1} from their gas-phase values, as anticipated of AD methanols.

When methanol is placed in a H-bond accepting solvent such as acetone-d_6, the ν_2 and ν_3 methanol methyl C−H stretches shift systematically to lower frequency as the acetone concentration is increased. A representative FTIR spectrum with 0.09 mole fraction methanol in acetone-d_6 is shown in Figure 6b), while the frequency shift data for a series of solution concentrations is summarized in Figure 7. At small concentrations of methanol in acetone (x(acetone) > 0.95) the OH stretch region of methanol (not shown) has shifted from a broad absorption centered at 3340 cm^{-1} to a much narrower band centered at 3507 cm^{-1}, characteristic of a donor methanol in a $CH_3OH\cdots O{=}C(CD_3)_2$ H-bond. This is close to the OH stretch fundamental assigned to the CH_3OH−acetone complex in an Ar matrix (3518 cm^{-1})[35] and provides strong evidence that most methanols in the dilute methanol/acetone solutions are involved in H-bond donation to acetone (i.e., as D methanols). Consistent with this transformation from AD to D, the ν_2 and ν_3 C−H stretch frequencies shift asymptotically (Figure 6b) to values 7.4 and 4.2 cm^{-1}, respectively, below their positions in pure liquid methanol (−30.4 and −14.9 cm^{-1} below their gas-phase values). A comparison of these shifts with the characteristic frequency shifts for the AD and D methanols in Figure 5 shows that, even in the condensed phase, the C−H stretch frequencies faithfully reflect the change in H-bonding environment from AD to D.

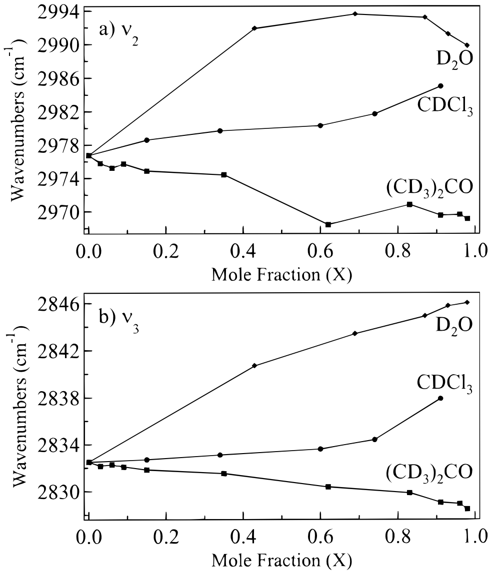

Figure 7. Frequencies for the (a) ν_2 and (b) ν_3 CH stretch fundamentals as a function of mole fraction of the indicated solvent X (where X = D_2O, $CDCl_3$, or acetone-d_6) in a binary liquid solution with methanol. Peak positions were obtained by fitting the band profiles to a sum of Gaussians. The observed shifts are consistent with a transformation of methanol from AD in pure liquid methanol to AAD in D_2O, A in $CDCl_3$, and D in acetone-d_6. See the text for further discussion.

A second example, involving mixed water/methanol solutions, tests the transformation of methanol from AD to AAD. At large dilution in water, a typical methanol molecule will take up a position in the tetracoordinated water network, accepting H-bonds from two water molecules and donating its single hydrogen to a methanol-to-water H-bond. As expected from Figure 5, under such circumstances, the methyl CH stretch fundamentals should shift characteristically to higher frequency by 10−20 cm^{-1} upon dilution in water. As can be seen from Figure 6c and Figure 7, this is exactly what is observed.

Finally, analogous scans of a series of solutions of methanol in $CDCl_3$ show a small shift toward higher frequency with increasing $CDCl_3$ mole fraction. $CDCl_3$, unlike acetone or water, can participate only as a weak donor in a $C{-}D\cdots O$ H-bond with methanol. While the magnitudes of the shifts are thereby necessarily small, the shifts to higher frequency in both ν_2 and ν_3 are consistent with a transformation of methanol from AD to A under such circumstances.

The combined FTIR data on methanol solutions with acetone-d_6, D_2O, and $CDCl_3$, then, indicate that the CH stretches of methanol can be used as a probe of methanol's average H-bonding environment even in the condensed phase.

V. Conclusions

RIDIR spectroscopy has been used to study the methyl C−H stretch fundamentals of methanol in different, known H-bonding environments produced by cold, gas-phase benzene−(methanol)$_m$ clusters with m = 1−5. The C−H stretch fundamentals of methanol's methyl group shift to characteristic frequencies that reflect the local H-bonding environment of the methyl group. Admittedly, the magnitudes of the C−H stretch frequency shifts are much smaller than those of the O−H stretch.

Nevertheless, the CH stretch shifts have several advantages over the O−H stretch, including (i) serving as a more localized probe of the H-bonding environment of each methanol, (ii) responding with similar sensitivity to acceptor and donor environments, and (iii) shifting to unique frequency regions associated with the occupation of the three H-bonding sites (two acceptor and one donor) of a given methanol molecule.

Acknowledgment. We gratefully acknowledge NSF for support of this research under CHE-9728636. C.J.G. thanks Lubrizol Corp. for fellowship support. The authors thank Prof. K. D. Jordan for carrying out electrostatic calculations on the methanol dimer, which probed the effect of H-bonding on donor and acceptor methyl groups.

References and Notes

(1) Pimentel, G. C.; McClellan, A. L. *The Hydrogen Bond*; W. H. Freeman: San Francisco, 1960.

(2) Coussan, S.; Loutellier, A.; Perchard, J. P.; Racine, S.; Peremans, A.; Tadjeddine, A.; Zheng, W. Q. *J. Chem. Phys.* in press.

(3) Huisken, F.; Kulcke, A.; Laush, C.; Lisy, J. M. *J. Chem. Phys.* **1991**, *95*, 3924−3929.

(4) Buck, U.; Ettischer, I. *J. Chem. Phys.* **1998**, *108*, 33−38.

(5) Hagemeister, F. C.; Gruenloh, C. J.; Zwier, T. S. *J. Phys. Chem. A* **1998**, *102*, 82−94.

(6) Pribble, R. N.; Hagemeister, F.; Zwier, T. S. *J. Chem. Phys.* **1997**, *106*, 2145−2157.

(7) Kabisch, G.; Pollmer, K. *J. Mol. Struct.* **1982**, *81*, 35−50.

(8) Mizuno, K.; Miyashita, Y.; Shindo, Y.; Ogawa, H. *J. Phys. Chem.* **1995**, *99*, 3225−3228.

(9) Huisken, F.; Stemmler, M. *Chem. Phys. Lett.* **1988**, *144*, 391−395.

(10) Buck, U.; Gu, X.; Lauenstein, C.; Rudolph, A. *J. Phys. Chem.* **1988**, *92*, 5561−5562.

(11) Huisken, F.; Stemmler, M. *Chem. Phys. Lett.* **1991**, *180*, 332−338.

(12) Buck, U.; Siebers, J.-G.; Wheatley, R. J. *J. Chem. Phys.* **1998**, *108*, 20−32.

(13) Page, R. H.; Shen, Y. R.; Lee, Y. T. *J. Chem. Phys.* **1988**, *88*, 5362−5376.

(14) Page, R. H.; Shen, Y. R.; Lee, Y. T. *J. Chem. Phys.* **1988**, *88*, 4621−4636.

(15) Frisch, M. J.; Trucks, G. W.; Schlegel, H. B.; Gill, P. M. W.; Johnson, B. G.; Robb, M. A.; Cheeseman, J. R.; Keith, T. A.; Petersson, G. A.; Montgomery, J. A.; Raghavachari, K.; Al-Laham, M. A.; Zakrzewski, V. G.; Ortiz, J. V.; Foresman, J. B.; Peng, C. Y.; Ayala, P. Y.; Chen, W.; Wong, M. W.; Andres, J. L.; Replogle, E. S.; Gomperts, R.; Martin, R. L.; Fox, D. J.; Binkley, J. S.; Defrees, D. J.; Baker, J.; Stewart, J. P.; Head-Gordon, M.; Gonzalez, C.; Pople, J. A. *Gaussian 94 (Revision B.3)*; Gaussian, Inc.: Pittsburgh, PA, 1995.

(16) Clark, T.; Chandrasekhar, J.; Spitznagel, G. W.; v. R. Schleyer, P. *J. Comput. Chem.* **1983**, *4*, 294.

(17) Hehre, W. J.; Ditchfield, R.; Pople, J. A. *J. Chem. Phys.* **1972**, *56*, 2257.

(18) Gruenloh, C. J.; Hagemeister, F. C.; Carney, J. R.; Florio, G. M.; Zwier, T. S. *J. Phys. Chem. A* **1999**, *103*, 503.

(19) Pribble, R. N.; Garrett, A. W.; Haber, K.; Zwier, T. S. *J. Chem. Phys.* **1995**, *103*, 531−544.

(20) Gruenloh, C. J.; Carney, J. R.; Hagemeister, F. C.; Arrington, C. A.; Zwier, T. S.; Fredericks, S. Y.; Wood, J. T.; Jordan, K. D. *J. Chem. Phys.* **1998**, *109*, 6601−6614.

(21) Zwier, T. S. *Annu. Rev. Phys. Chem.* **1996**, *47*, 205−241.

(22) Garrett, A. W.; Severance, D. L.; Zwier, T. S. *J. Chem. Phys.* **1992**, *96*, 7245−7258.

(23) Garrett, A. W.; Zwier, T. S. *J. Phys. Chem.* **1992**, *96*, 9710.

(24) Wang, X.; Ma, Y.; Chirokolava, A.; Perry, D. S. High-resolution infrared spectra of the ν_9 and $2\nu_4$ bands in methanol. 53rd Ohio State University International Symposium on Molecular Spectroscopy, 1998, Columbus, Ohio.

(25) Xu, L. H.; Wang, X. L.; Cronin, T. J.; Perry, D. S.; Fraser, G. T.; Pine, A. S. *J. Mol. Spectrosc.* **1997**, *185*, 158−172.

(26) Halonen, L. *J. Chem. Phys.* **1997**, *106*, 7931−7945.

(27) Hunt, R. H.; Shelton, W. N.; Cook, W. B.; Bignall, O. N.; Mirick, J. W.; Flaherty, F. A. *J. Mol. Spectrosc.* **1991**, *149*, 252−256.

(28) Bignall, O. N.; Hunt, R. H.; Shelton, W. N. *J. Mol. Spectrosc.* **1994**, *166*, 137−146.

(29) Serrallach, A.; Meyer, R.; Gunthard, H. H. *J. Mol. Spectrosc.* **1974**, *52*, 94−129.

(30) Fraser, G. T.; Lovas, F. J.; Suenram, R. D. *J. Mol. Spectrosc.* **1994**, *167*, 231−235.

(31) Buckingham, A. D. *Proc. R. Soc. London, Ser. A* **1958**, *248*, 169.

(32) Buckingham, A. D. *Proc. R. Soc. London, Ser. A* **1960**, *255*, 32.

(33) Buckingham, A. D. *Trans. Faraday Soc.* **1960**, *56*, 753.

(34) Wallen, S. L.; Palmer, B. J.; Garrett, B. C.; Yonker, C. R. *J. Phys. Chem.* **1996**, *100*, 3959−3964.

(35) Han, S. W.; Kim, K. *J. Phys. Chem.* **1996**, *100*, 17124−17132.